

## SELECTION OF SEISMIC ACCELERATION FOR NON-LINEAR ANALYSIS OF RC BUILDINGS IN BANGLADESH

**M.F. Haque\***

*Department of Civil Engineering, Bangladesh University of Engineering and Technology, Dhaka-1000,  
Bangladesh*

Received: 13 February 2022

Accepted: 24 June 2023

### ABSTRACT

*Seismic acceleration selection is a vital issue of non-linear time history analysis for reinforced concrete (RC) buildings. The propagation characteristic of selected seismic acceleration through soil medium depends on the material properties of the soil and reflected waves from the structure are absorbed by the adjacent soil medium. Stiffnesses of structural members are degraded by exciting and internal waves because of storing the hysteretic strain energy inside structural members. However, this study proposes a finite element model for the selection of seismic acceleration considering specific site classes in Bangladesh based on the soil stratum because seismic excitation varies with the site class. In addition, the structural response depends on the selected acceleration, and non-linear time history analysis represents the more reliable inelastic response of the structure due to this acceleration. Variation of seismic storey drift within allowable limit indicates appropriate selection of the seismic acceleration by the non-linear response history analysis. Also, lower rates of output acceleration intensities for upper stories may inform the majority of reflected waves absorbed by the soil medium. For this reason, proper selection of seismic acceleration may enhance the accurate non-linear response of RC buildings in Bangladesh.*

**Keywords:** *Direct Time Integration, Non-Linear Time History, Reinforced Concrete, Seismic Acceleration, Seismic Drift.*

### 1. INTRODUCTION

Non-linear time history analysis depends on the selected seismic acceleration and the structural inelastic response is confirmed by this analysis. Also, this analysis informs the amount of strain energy stored in the structural members. However, the structural responses of reinforced concrete members were influenced by the height variations of the structure with the various seismic excitations, and it was related to the amount of strain energy stored inside the structural members (Lin *et al.*, 2013). Non-linear time history analysis summarized those scenarios. Sometimes, seismic acceleration is matched with the specific response spectrum and the matching parameters are scaled by the standard. The reinforced concrete building shows various characteristics during response spectrum analysis. So, story drift is varied by variations of site classes. The worst site class showed a larger story drift (Chandak, 2012). During dynamic analysis, structural drift is varied with the material properties of members, and non-linear hinges are dependent on the arrangements of transverse reinforcement of beams. In addition, the non-linear time history analysis impacts the plastic hinge behaviors. The ductility of beams was varied by arrangements of reinforcements and reflected the material stiffness due to the occurrence of seismic excitation (Chen and Hsu, 2004). In some cases, joints of the structural members show brittle behavior because of the inadequate arrangement of ties. So, joints are failed first during seismic excitation. Pushover analysis provided reliable joint behaviors against lateral loads, and the joint failure mechanism was evaluated by the non-linear static analysis (Dinar *et al.*, 2014). Linear, non-linear, dynamic, and static analyses are related to the fundamental period of the structure. The period of the concrete and steel structures was evaluated using trial and error methods (Haque, 2021). The performance of reinforced concrete floating columns was predicted by the non-linear time history analysis during seismic excitation, while the vertical component of seismic excitation showed higher performance than the horizontal component (Narsing and Sharma, 2016). The performance of low-rise buildings was observed at higher compared to the high-rise building from the response spectrum analysis, and structures with infilled walls represented lower drift than those without infilled (Patil and Pawar, 2020). Response of masonry buildings was predicted to be lower compared to the reinforced concrete building because of the confinement of ductile steel with brittle concrete (Pauley and Priestly, 1992). Non-linear time history analysis evaluated the stiffness degradation mechanism, which showed more realistic behaviors than simple pushover analysis. For this reason, the container crane showed hysteretic behavior under the non-

\*Corresponding Author: [mfh.civil@gmail.com](mailto:mfh.civil@gmail.com)

<https://www2.kuet.ac.bd/JES/>

ISSN 2075-4914 (print); ISSN 2706-6835 (online)

linear time history analysis (Tran *et al.*, 2018). However, non-linear time history analysis is more effective for the analysis of structures than other numerical analyses. Acceleration is the function of time and the inelastic response of structure depends on the amount of strain energy stored by the structural members. This energy is measured by the non-linear time history analysis. Acceleration selection is the major part of the non-linear response history analysis. This acceleration is selected by matching the time history function (El Centro 1940 earthquake) with the response spectrum of the specific site class of SC according to the Bangladesh National Building Code (BNBC, 2020). For this reason, non-linear finite element analysis is performed in this study to predict the response of structure for the selected acceleration.

## 2. CONSIDERATIONS OF THE PROPOSED NUMERICAL MODEL

In this study, 15 storied reinforced concrete L-shaped model is proposed for the numerical analysis by ETABS 18.1.1. Shapes of beams, columns, and slabs are considered to be rectangles and all structural members maintain unique sizes. Figure 1 represents the details geometric properties of the proposed model. The support condition of this structure is considered to be spring, and two types of springs are attached to the support such as static and dynamic. Also, spring stiffness is provided in three orthogonal directions. Supports with springs are represented in Figure 2. The 3D view of this structure is represented in Figure 3. There are four types of analysis conducted for this structure such as linear static, response spectrum, linear time history, and non-linear time history. During these analyses; beams and columns are considered to be two noded line elements. In addition, slabs are taken to be four noded rectangular elements. Gauss integration rule is applied for the numerical integration. The Newmark method is considered to perform the dynamic analysis. However, iteration is continued until convergence will be achieved for non-linear analysis. Static subgrade modulus ( $k_s$ ) is represented by Eq. (1). The ultimate bearing capacity of the soil ( $q_{ult.}$ ), soil settlement of the ultimate load ( $\Delta H$ ), and area of the square footing ( $A_F$ ) are considered to be 43 kN/m<sup>2</sup>, 25.4mm, and 2.25m<sup>2</sup>, respectively. Dynamic spring stiffnesses such as horizontal ( $k_y$ ), vertical ( $k_z$ ), rocking ( $k_{\theta x}$ ), and torsional ( $k_t$ ) modes are expressed by Eq. (2), Eq. (3), Eq. (4), and Eq. (5), respectively. These stiffnesses are the functions of the shear modulus (G) of the soil, width (B) of the footing, and Poisson's ratio ( $\mu$ ) of the soil.

$$k_s = k_x = k_y = k_z = q_{ult.}A_F / \Delta H \quad (1)$$

$$k_y = 8GB / (1 - \mu) \quad (2)$$

$$k_z = 4GB / (1 - \mu) \quad (3)$$

$$k_{\theta x} = 8GB^3 / 3(1 - \mu) \quad (4)$$

$$k_t = 16GB^3 / 3 \quad (5)$$

Geometric properties along with dimensions of this structure are represented in Figure 1. Foundations are considered to be single-isolated. Material properties of all elements of this structure are considered to be the same. The cylindrical compressive strength of concrete is taken to be 21 MPa. Also, Poisson's ratios of steel, concrete, and soil are assumed to be 0.30, 0.20, and 0.45, respectively. The yield strength of steel is taken to be 415 MPa. In addition, the expected yield and tensile strengths of steel are considered to be 1.1 and 1.5 times of original yield strength of steel. The elastic stiffness of spring in three directions is taken to be 3809 kN/m. Also, dynamic spring stiffnesses of vertical, horizontal, rocking, and torsional modes of the base of this structure are estimated to be 80973894 kN/m, 57465344 kN/m, 121460840 kN-m/rad, and 133606924 kN-m/rad, respectively. These spring stiffnesses are depended on the footing dimensions and material properties of the soil. In this study, the modulus of elasticity of soil and concrete is considered to be the same, and the coarse aggregate of concrete is considered to be stone chips. Live and extra dead loads of all floors except the roof are considered to be 5 kN/m<sup>2</sup> and 3 kN/m<sup>2</sup>, respectively. Roof live and extra dead loads are taken to be 1.5 kN/m<sup>2</sup> and 1 kN/m<sup>2</sup>, respectively. On the ground floor, only peripheral beams carry uniformly distributed loads such as 7.3 kN/m. Similarly, loads on the roof peripheral beams are taken to be 2.9 kN/m. Other beams of this structure carry a uniformly distributed load of 7.3 kN/m. The seismic load of this structure is calculated by the equivalent static method for linear elastic analysis (BNBC, 2020). Soil settlement at ultimate load is considered to be 25.4 mm and it is used for the calculation of elastic spring stiffness. In reality, some of the buildings are seen to be L-patterns and in most cases, the center of mass or rigidity is standing outside this shape. For this reason, the seismic response of this structure is more critical than other shapes such as rectangles, trapezoidal, squares, etc. Therefore, the present research proposes an L-shape structure to predict seismic response by various analysis techniques. A concrete hysteresis material model is used for the non-linear analysis (ETABS, 2017). In this

model; tension and compression behaviors are independent and behave differently. The energy degradation factor,  $f$  is specified for this model. This value should satisfy  $0 \leq f \leq 1.0$ . A value of  $f = 0$  is equivalent to a clean gap when unloading from compression and dissipates the least amount of energy. A value of  $f = 1.0$  dissipates the most energy and could be caused by rubble filling the gap when unloading from compression.

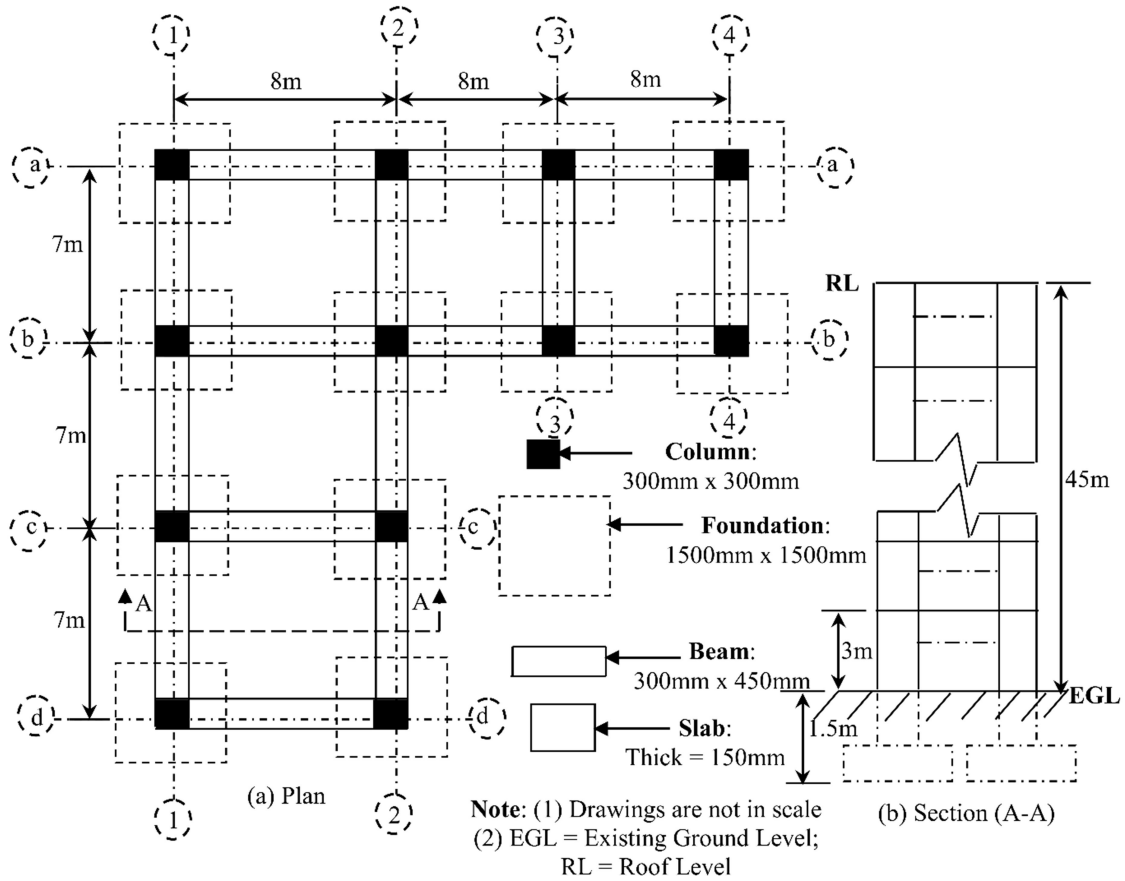


**Figure 1:** Geometric properties of the proposed numerical model.

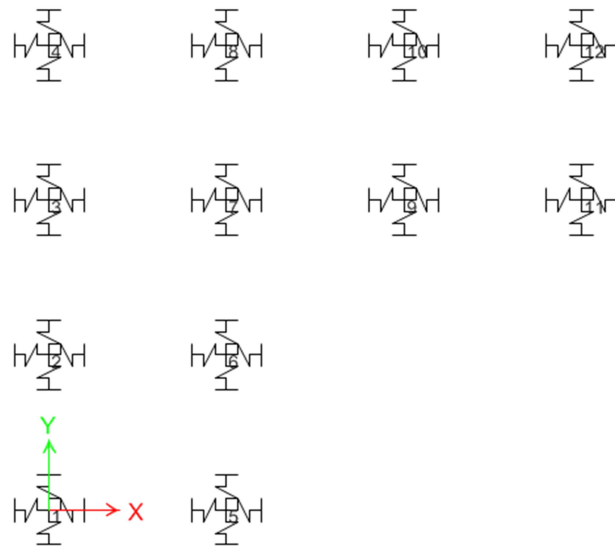


**Figure 2:** Layout of support springs.

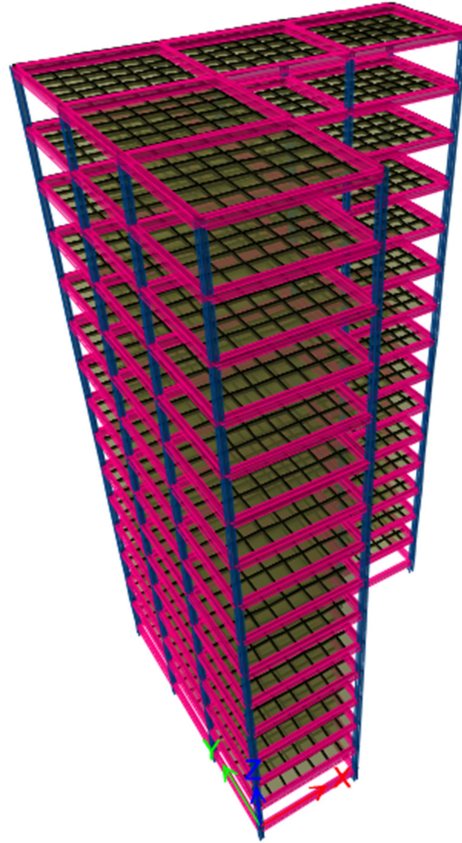


**Figure 3:** 3D meshed view of the proposed 15-storied building.

### 3. METHODOLOGY OF VARIOUS ANALYSIS TECHNIQUES OF THE PROPOSED MODEL

The analysis procedure of different methods is varied. Four analysis methods are addressed in this study. Parameters for these analyses are taken based on the Bangladesh National Building Code (BNBC, 2020). The selection of seismic acceleration is necessary for non-linear time history analysis because the performance of the structure is evaluated by this analysis. This acceleration depends on the site class when the response spectrum is matched with any location's time history data because of the unavailability of seismic records at the specified site. In this study, the response spectrum of the SC site class is matched with the EI Centro 1940 earthquake data. A matching function is used for time-history analysis.

#### 3.1 Linear Static Analysis

In this analysis; dead, superimposed dead, and unreduced live loads are applied in the structure along the direction of gravity. Seismic loads in both lateral directions of the structure are assigned by using coefficients. These coefficients are calculated by using formulae for the SC site class. An equivalent static procedure is followed for this calculation (BNBC, 2020). No live load is added for the calculation of static seismic force. The assignment of seismic load in the structure is represented in Table 1. Seismic force is applied from the base to the roof level of the structure. 5% eccentricity is considered for all diaphragms in both directions because of different locations of mass and rigidity centers. All dead loads are added to the mass source with a unit scale factor in ETABS. Linear static analysis is the initial stage of other advanced analyses.

**Table 1:** Considerations and parameters of the seismic loading for the linear static analysis.

Items	Remarks
Method of seismic loading	User coefficient
Application directions	Two horizontal at the base
Diaphragm eccentricity	Five percent
Base shear coefficient	0.0322
Building height exposure	1.465
Story range	From base to 15 <sup>th</sup> floor

### 3.2 Response Spectrum Analysis

Response spectrum analysis is the superposition of modal analysis. The modal analysis is performed for the eigen cases. The maximum number of modes of this structure is set to be 90 because each story consists of six modes such as four translational and two rotational. In this structure exists the P-delta option. So, the iterative load-based P-delta effect is added to the modal cases. Considerations of modal and response spectrum analysis are represented in Table 2. The response spectrum curve is generated by using the formulations of the Bangladesh National Building Code (BNBC, 2020). The input response spectrum of this structure is expressed in Figure 4. This spectrum is plotted for the maximum time of four second period. Modal combination and directional combination during response spectrum analysis are considered to be CQC and SRSS. Constant 5% modal damping is assumed for all modes and the scale factor is the function of some parameters such as structure importance coefficient, gravitational accelerations, and response reduction coefficient. These parameters are selected for the SC site class. In addition, the seismic zone factor and design category of this building is considered to be 0.20 and C, respectively (BNBC, 2020).

**Table 2:** Parameters for the modal and response spectrum analysis.

Parameters	Remarks
Modal case	Eigen
Maximum number of modes	90
Minimum number of modes	1
Direction of acceleration	Two orthogonal in the horizontal plane
Modal combination method	Complete Quadratic Combination (CQC)
Directional combination type	Square root sum of squares (SRSS)
Modal damping	0.05

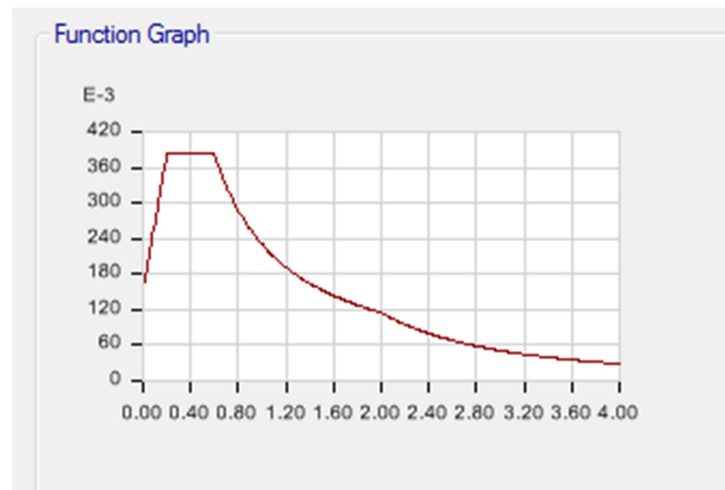


**Figure 4:** Input response spectrum for SC site class.

### 3.3 Linear Time History Analysis

EI Centro 1940 earthquake data is scaled by the response spectrum curve by using a standard (BNBC, 2020). The scaled-matched function is used for the time history function during analysis. The input-matched time history function is shown in Figure 5. The total time of seismic shaking is considered to be 4 seconds and the output time step is taken as 0.05 seconds. Parameters for linear time history analysis are expressed in Table 3.

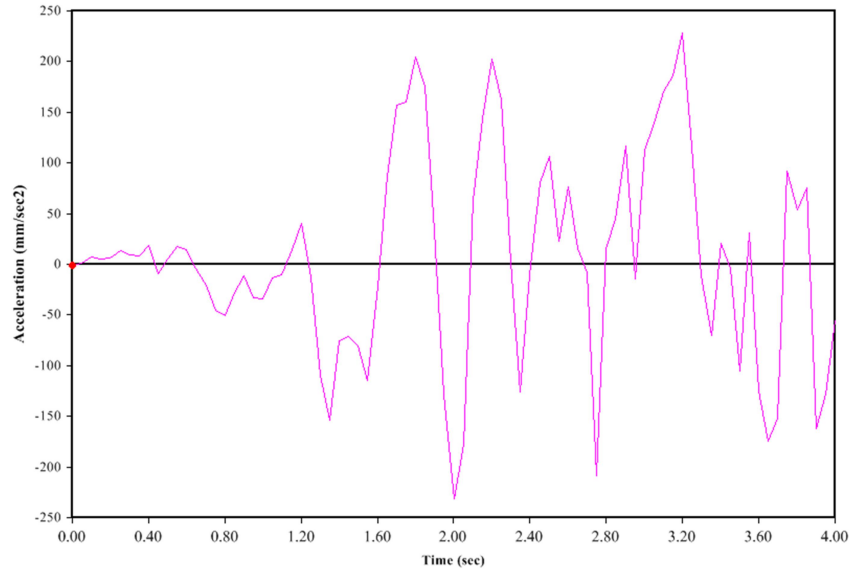


**Figure 5:** Input matched time history function for analysis.

**Table 3:** Linear time history analysis parameters.

Parameters	Remarks
Integration type	Linear direct
P-Delta settings	Iterative based on loads
Acceleration directions	Two orthogonal in the horizontal plane
Number of output time step	80
Output time step size	0.05 second
Time integration	Newmark

**3.4 Non-Linear Time History Analysis**

In non-linear time history analysis, plastic hinges are provided at beams and column joints based on the standard (ASCE 41-13, 2014). Because there has been no information about plastic hinges in Bangladeshi standards (BNBC, 2020). Base shear is taken along the Y-directional seismic force for the selection of hinges. Also, transverse reinforcements are considered for the hinges of beams. Parameters for the non-linear time history analysis are represented in Table 4. The isotropic hysteresis parameter is considered for concrete and steel. In the non-linear process, analysis is conducted by the direct integration method, and the P-delta option is switched off for this case because of satisfying the drift of limiting value at the end of linear time history analysis.

**Table 4:** Parameters and considerations for the non-linear time history analysis.

Parameters	Remarks
Auto hinge type	ASCE 41-13
Hinge table for concrete column	Table 10-8
Interaction	P-M2-M3
Load combination	Service plus earthquake
Concrete column failure condition	Flexure or Shear
Shear reinforcing ratio	Based on the current design
Deformation controlled hinge load carrying capacity	Drops load after point E
Hinge table from beam	Table 10-7
Degree of freedom	Moment in major direction
Transverse reinforcing	Active
Rebar grade	415 MPa
Hysteresis type	Isotropic
Stress-strain curve type for rebar	Simple
Acceptance Criteria of Strains for rebar in tension	Immediate Occupancy (IO): 0.01, Life Safety (LS): 0.02, Collapse Prevention (CP): 0.05
For rebar, strain at onset of strain hardening, ultimate strain capacity, and final slope (multiplier on E)	0.01, 0.09, and -0.1

Parameters	Remarks
Crushing strength of concrete materials (beam, column, slab, footing)	21 MPa
Drucker-Prager parameters of friction and dilatational angle	Zero degree
Tensile strain of concrete material	Ignore acceptance criteria
Stress-strain curve type for concrete materials	Mander
Acceptance Criteria of Strains for concrete materials in compression	IO: -0.003, LS: -0.006, CP: -0.015
For concrete materials, strain at onset of strain hardening, ultimate strain capacity, and final slope (multiplier on E)	0.002219, 0.005, and -0.1
Time dependent type	ACI 209R-92
Time dependence consideration	Compressive strength and stiffness (Modulus of Elasticity)
Creep analysis type	Full integration
Compressive strength factor, $\alpha$ and $\beta$	2.3 and 0.92
Integration type	Non-linear direct integration
Initial condition	Start from unstressed state
Acceleration directions	Two orthogonal in the horizontal plane
Number of output time step	80
Output time step size	0.05 second
Time integration type	Newmark

#### 4. RESULTS AND DISCUSSION

Linear static, response spectrum, linear time history, and non-linear time-history analyses evaluate the overall performance of the structure under selected seismic excitation. Some intensities of seismic force are absorbed by the soil medium. Support springs express these phenomena. The response of this structure is finalized by the performance of drift. In addition, material properties are influenced by structural performance. Some similarity is found with this study from the existing literature. A study was performed to select seismic excitation by non-linear time history analysis by using the response spectrum for Vancouver, Canada (Lin *et al.*, 2012). Three reinforced concrete buildings were studied and the number of stories was 4, 10, and 16. Scaled, modified, simulated, and artificial accelerograms were used in that study as input motion. The story shears, inter-storey drift, and curvature were recorded in that study to predict responses of the reinforced concrete buildings. According to the analysis results, the scaled accelerogram is recommended to use in time history analysis for the reinforced concrete frame building. In this study, some of the important results are recorded to express the response of the reinforced concrete structures under the selected seismic acceleration.

##### 4.1 Irregularities of Structure

Structural irregularities are checked for linear static analysis, but it is no big problem with the existence of irregularities. Because response spectrum and time history analyses optimize irregularities. In this structure, re-entrant corner irregularity exists; all irregularities are shown in Table 5.

**Table 5:** Structural irregularities check based on the linear static analysis.

Types of irregularities	Remarks
Torsional	Not exist
Re-entrant corner	Exist
Diaphragm discontinuity	Not exist
Out-of-plane offsets	Not exist
Non-parallel system	Not exist
Soft-storey	Not exist
Mass	Not exist
Vertical geometric	Not exist
Vertical in-plane discontinuity	Not exist
Weak-storey	Not exist

#### 4.2 P-Delta Effect of Structure

P-Delta is the second-order effect on the structure and it is contributed to linear and non-linear cases. During P-Delta analysis; coefficients of the effective moment of inertia of beams, columns, and slabs are considered to be 0.35, 0.7, and 0.25, respectively (BNBC, 2020). The slab can't take any moment from the beam in first-order analysis. P-Delta effects for this structure are represented in Table 6. The stability coefficient of each storey exceeds the code (BNBC, 2020) prescribed limiting value of 0.10. So, the load-based iterative P-Delta effect is included with the modal, response spectrum, and linear time history cases except for non-linear time history analysis. Because P-Delta-induced storey drift is recovered at the end of the linear time history analysis.

**Table 6:** P-Delta checks of the structure in the direction (Y) of maximum drift of linear static analysis.

Number of stories	Unfactored gravitational load (kN)	Drift (mm)	Lateral storey shear (kN)	Stability coefficient	Remarks
1	46052	145	1516	0.33	Exist
2	42903	141	1508	0.30	Exist
3	39755	141	1492	0.28	Exist
4	36606	141	1465	0.26	Exist
5	33458	140	1426	0.24	Exist
6	30309	138	1375	0.23	Exist
7	27161	137	1308	0.21	Exist
8	24013	135	1227	0.20	Exist
9	20864	131	1128	0.18	Exist
10	17716	129	1013	0.17	Exist
11	14567	125	879	0.15	Exist
12	11419	120	726	0.14	Exist
13	8270	116	554	0.13	Exist
14	5122	110	360	0.12	Exist
15	1974	105	146	0.11	Exist

#### 4.3 Accelerations Spectrums

Seismic excitation is attacked at each joint of the structure. So, the joint accelerations spectrums control the response of the structure due to the non-linear time history analysis. Joint levels of this structure are expressed in Figure 6. The maximum acceleration spectrum is located at the base level. Each joint of this level shows the same acceleration spectrum for 5% modal damping. Similarly, the minimum acceleration spectrum is located on the 14<sup>th</sup> floor of joint 1 in the Y-direction because the effect of the seismic shaking is reduced along with the building height due to the successive plastic hinge formation on the members of the lower stories of the structure by the degradation of the hysteresis loop. Maximum and minimum accelerations spectrums are represented in Figure 7 and Figure 8, respectively. The value of the 5% modal damping containing the maximum acceleration spectrum is exceeded from the input maximum selected acceleration for the SC site class. Also, the minimum acceleration spectrum value is less than the input value. So, non-linear time history analysis better perform for this case. In non-linear time history analysis, base shear is maximum at 3.4 seconds of seismic excitation and the variations of base shear are represented in Figure 9. Accelerations are varied along with the storey height and the magnitudes of these variations are less than from input acceleration except for acceleration at the base. Absolute acceleration variations along the height of the structure for X and Y directions are represented in Figure 10. These variations show better performance of the structure under selected seismic acceleration.



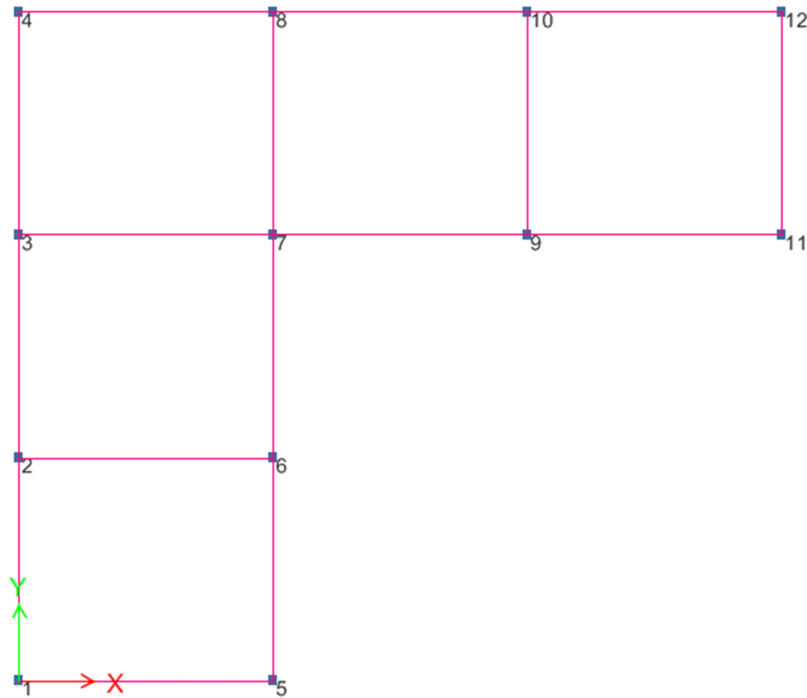


Figure 6: Various joints of the proposed model.

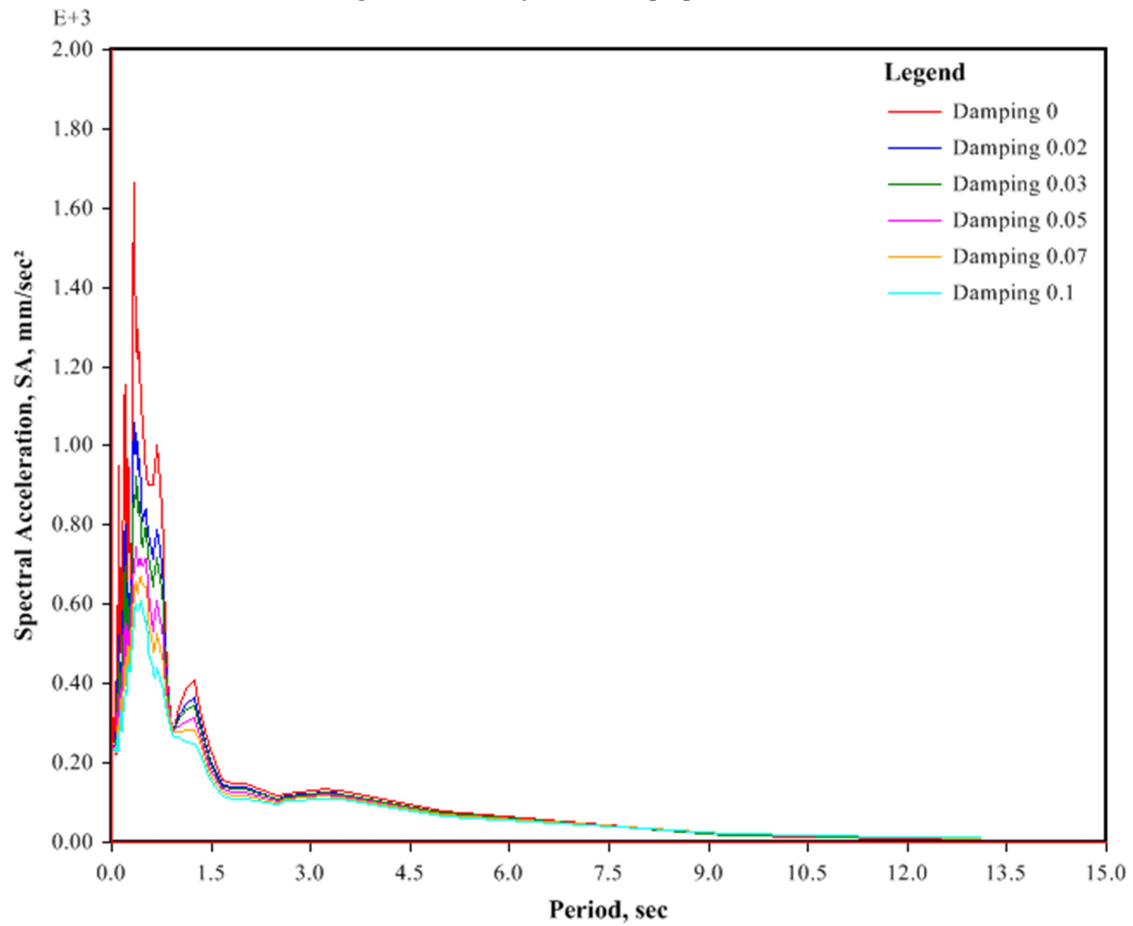
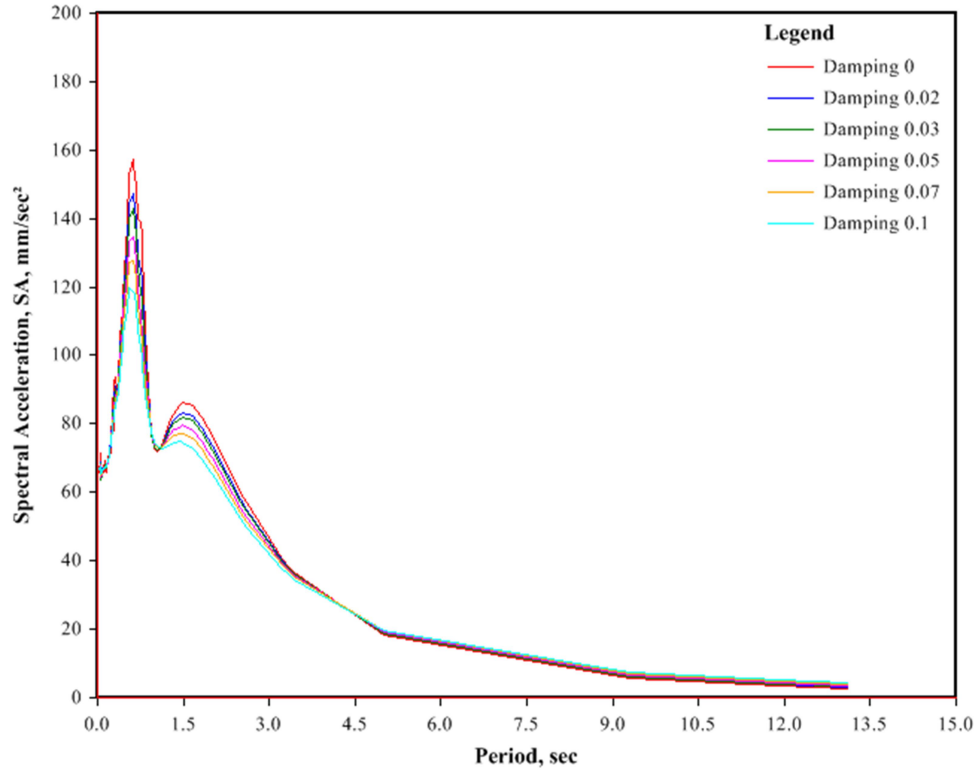
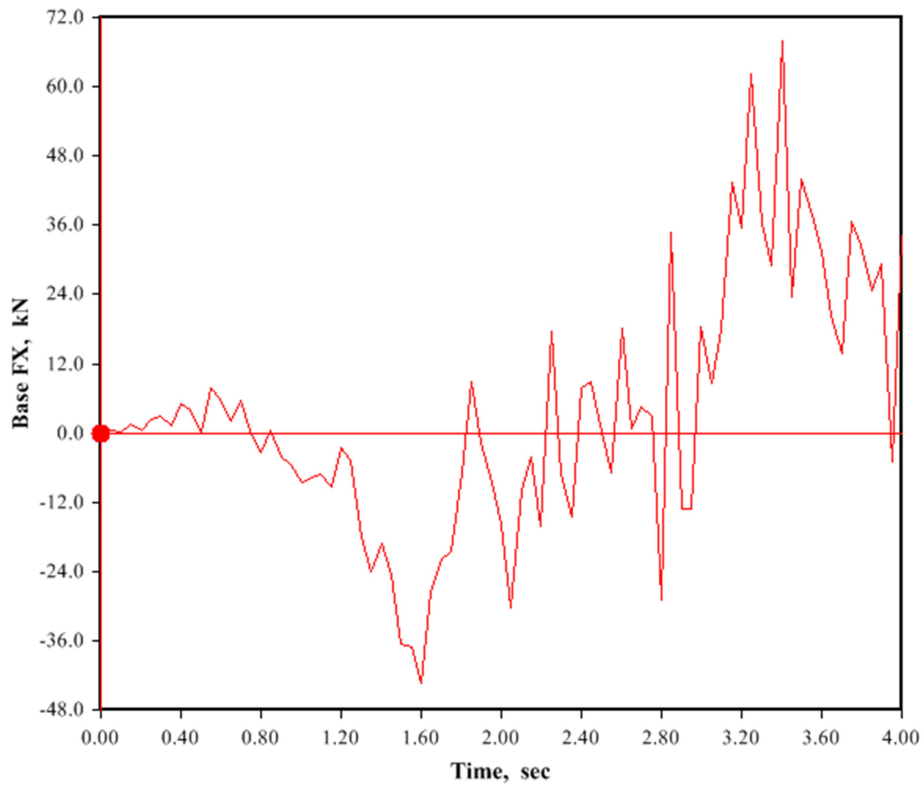


Figure 7: Maximum acceleration spectrum at the base level.



**Figure 8:** Minimum acceleration spectrum at 14<sup>th</sup> floor level of joint 1 in Y-direction.



**Figure 9:** Variations of base shears with the time of selected acceleration.

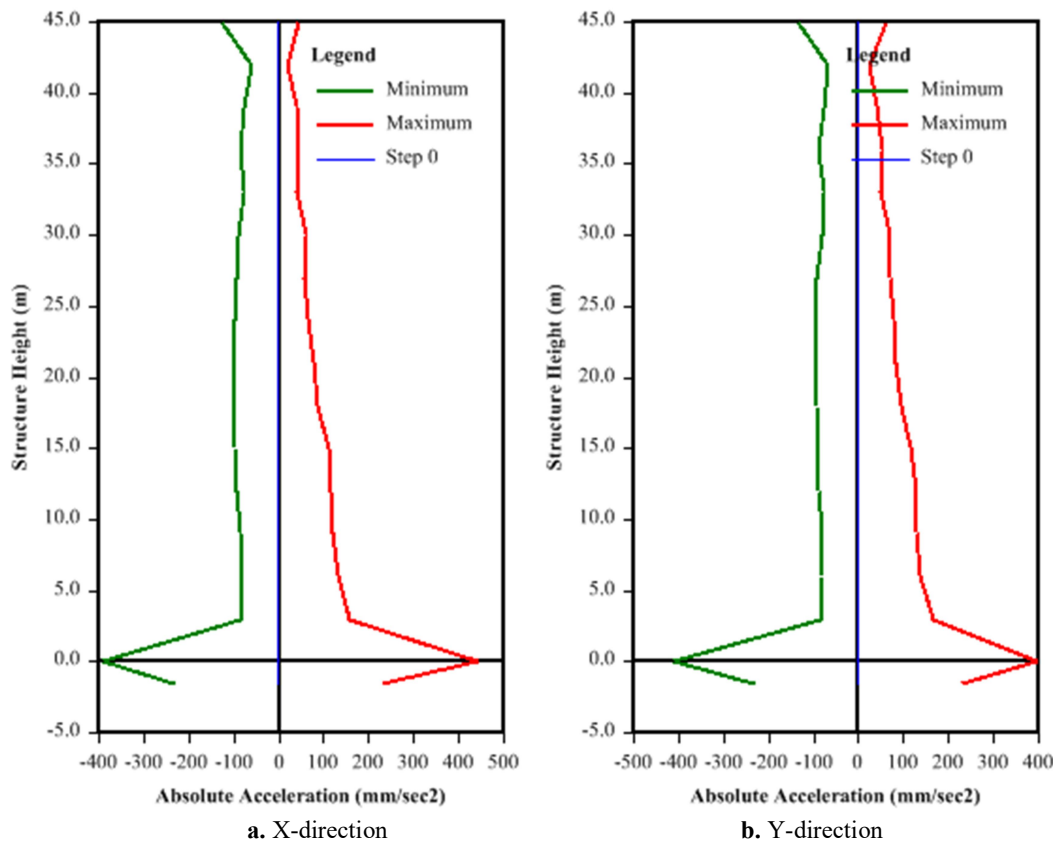


Figure 10: Variations of absolute accelerations along the storey height of the proposed model.

#### 4.4 Variations of Drifts

Drifts are varied along with the number of stories whereas lower stories represent higher drift because of lower seismic excitation of higher stories due to the loss of the residual stress by the degradation of the hysteresis loop during the non-linear time history analysis. In reality, seismic excitation is absorbed by the lower storey first for the damping properties of the structure then it is decreasing with the increment of the story height. So, inter-storey drift is reduced. In addition, the linear static analysis represents higher drift which exceeds the code (BNBC, 2020) prescribed limiting and extreme values. Linear and non-linear time history analyses express lower drift within its limit because of releasing strain energy of the structural members for the degradation of the hysteresis loop during the time history analysis. Although the difference in these drifts variations are close to each other, which are shown in Figure 11 and Figure 12. In addition, non-linear time history analysis represents the lowest drift because of the losses of the residual stress of successive iteration stages. Drift is a vital issue to evaluate the performance of the structure under seismic excitation. Drifts of the X and Y directions of this structure are very close to each other. In response spectrum analysis (RSA), linear time history analysis (LTHA), and non-linear time history analysis (NTHA), design drift (DD) is obtained by the multiplications of software-prescribed numerical value with the code (BNBC, 2020) prescribed displacement amplification factor. However, the minimization of drift value represents an optimization of the load-deflection effect on the structure. Drift for the linear static analysis (LSA) exceeds the code-prescribed limiting drift (LD) and extreme drift (ED) in the X and Y directions of the structure but the difference between the two directional drifts for the LSA is less than 15%. In both directions (X and Y) of the structure, drifts are stood within the extreme level drift except the drifts of the LSA and some portions of the design drift of RSA because of no strain energy release due to the LSA and RSA to degrade the hysteresis loop.

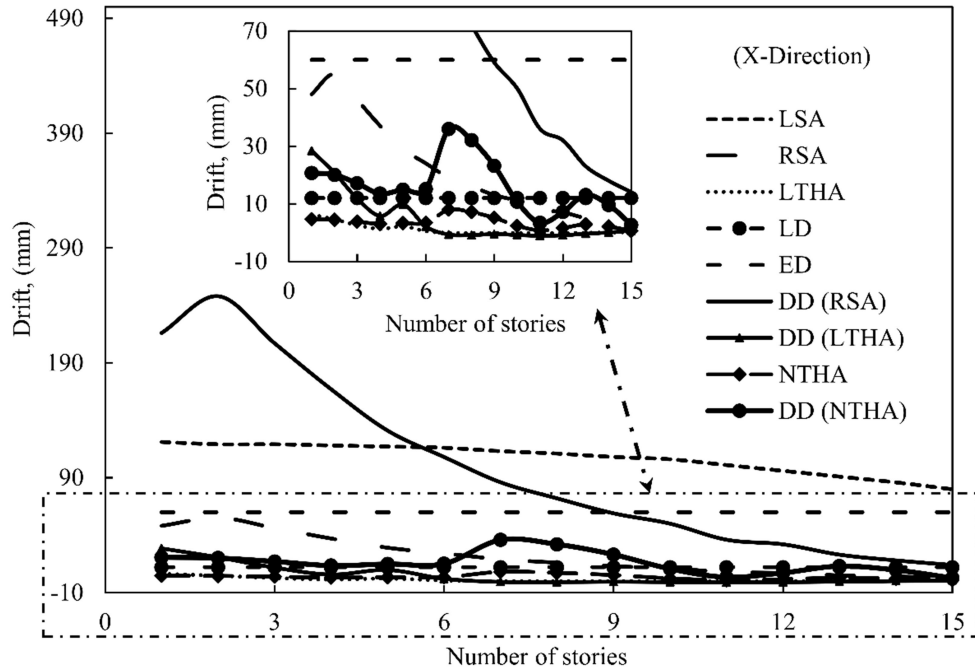


Figure 11: Variations of drifts in the X-direction of the proposed model.

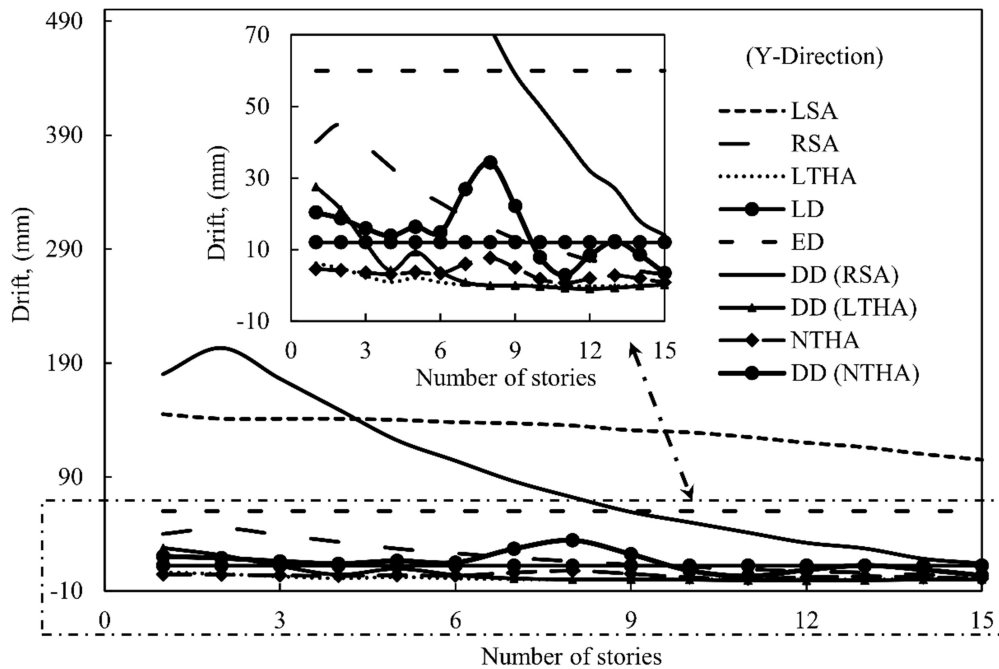


Figure 12: Variations of drifts in the Y direction of the proposed model.

5. VALIDATION OF ETABS 18.1.1

This study is performed by numerical analysis using ETABS 18.1.1. So, it is necessary to validate this numerical package with the previous (Patil and Pawar, 2020) numerical research. G+3 infilled wall structural model is considered to be the numerical analysis for validation purposes. That building was regular in shape and the width of the infilled wall was 424mm. The yield strength of steel and cylindrical compressive strength of concrete was 415 MPa and 20 Mpa, respectively. Unit weights of beams, columns, and slabs were 25 kN/m<sup>3</sup> and it was 20 kN/m<sup>3</sup> for the infilled wall. Poisson’s ratio of concrete was 0.20. The depth and width of the beam were 380mm and 250mm, respectively. Also, the width and depth of the column were 250mm and 380mm. The thicknesses of the slab and infilled wall were 150mm and 250mm, respectively. Both directions carried three

bays and the width of each bay was 4m. Therefore, the geometric plan and 3D view of the validation model are represented in Figure 13 and Figure 14, respectively. Response spectrum analysis was performed by considering Indian standards. So, the input response spectrum is represented in Figure 15. Based on the re-analyzed results, the fundamental period and base shear of this structure is close to the previous study but some difference shows the results of maximum displacement and drift. Validation results are shown in Table 7. Differences in results between the present and previous studies for the time period, base shear, maximum displacement, and maximum drift are 11.6%, 8.7%, 10%, and 13.8%, respectively. Therefore, lower differences in results may convince the accuracy of the finite element code of ETABS 18.1.1.

**Table 7:** Validation results of response spectrum analysis for infilled G+3 building.

Identification	Time period (second)	Base shear (kN)	Maximum displacement (mm)	Maximum drift (mm/mm)
Patil and Pawar, 2020	0.172	184.4	0.0461	0.0000050
Present study (ETABS 18.1.1)	0.152	168.4	0.0512	0.0000058

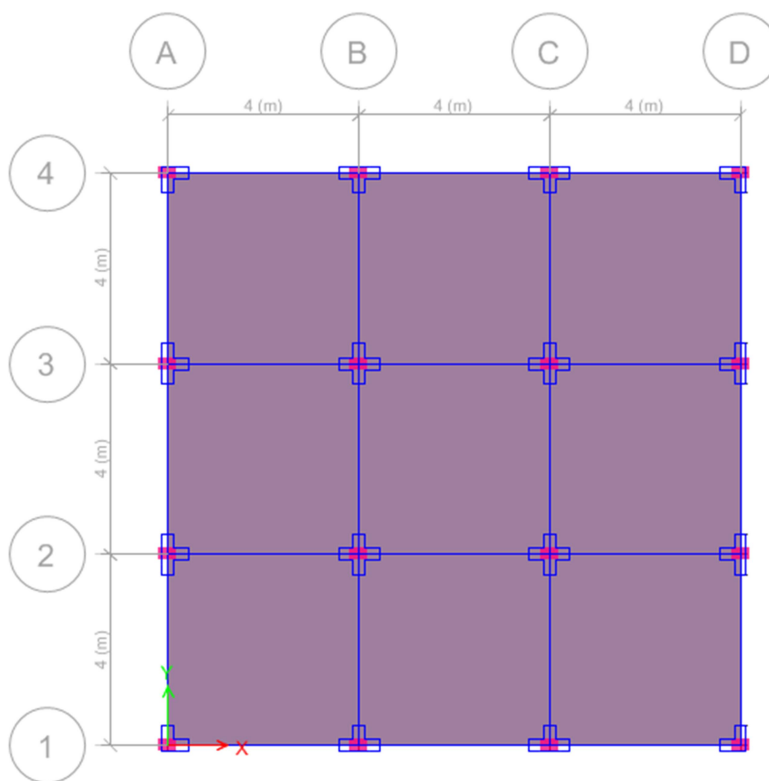


**Figure 13:** Plan of the validation model.

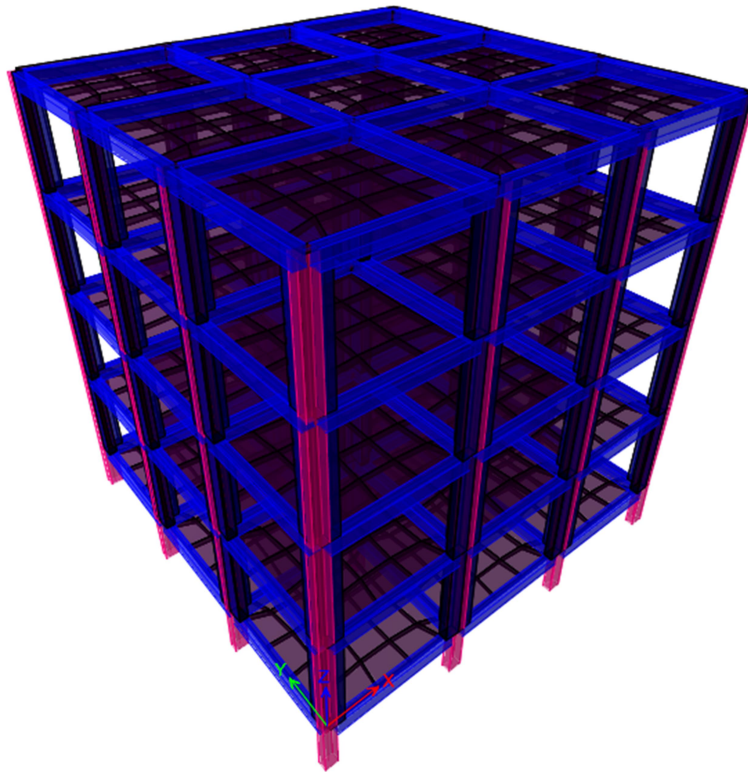


Figure 14: 3D view of the validation model.

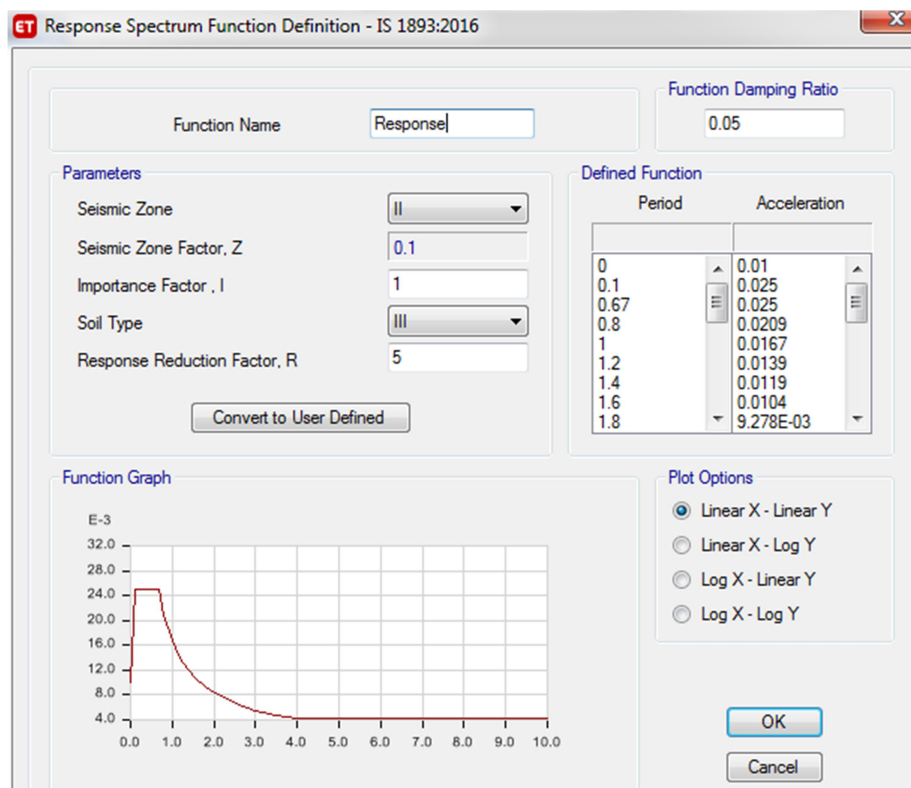


Figure 15: Input response spectrum of the validation model.

## 6. CONCLUSIONS

Seismic acceleration is related to the individual performance of the structural member. It impacts the response of the total structural system. Therefore, major findings are summarized herewith based on the numerical analysis results according to the objectives of this study.

- Non-linear time history analysis is dependent on the seismic acceleration function, and it minimizes seismic drift. Soil characteristics of the structure are controlled by drift. Because the soil is sufficient radiation-damping properties. on the other hand, the response spectrum is produced based on the soil properties. Also, this spectrum is controlled by the time history, when it is matched with the time history.
- In Bangladesh, there has no sufficient amount of heavy earthquake data. So, site specified response spectrum is matched with the EI Centro 1940 earthquake data for the selection of the acceleration-induced time history function. Because this selected site class-induced acceleration reflects the overall structural performance of the proposed model. In addition, acceleration-induced drift is a vital issue for the structural response of the present numerical model.
- The drift of this proposed model is minimized after completion of the non-linear time history analysis, and joint acceleration is less than the selected matched input acceleration. In addition, hysteresis behaviors of structural members represent the absorption capacity of selected seismic acceleration. Therefore, site specified selected acceleration for non-linear analysis in Bangladesh is suitable based on the structural performance of the proposed model.

## REFERENCES

- ASCE 41-13, 2014. Seismic Evaluation and Retrofit of Existing Buildings. *American Society of Civil Engineers*.
- BNBC, 2020. Bangladesh National Building Code. *Dhaka: Ministry of Housing and Public Works*.
- Chandak, N., 2012. Response Spectrum Analysis of Reinforced Concrete Buildings. *Journal of The Institution of Engineers (India): Series A*, Volume 93, pp. 121-128.
- Chen, C. C. & Hsu, S. M., 2004. Formulas for curvature ductility design of doubly reinforced concrete beams. *Journal of Mechanics*, 20(4), pp. 257-265.
- Dinar, Y., Hossain, I., Biswas, R. K. & Rana, M., 2014. Descriptive Study of Pushover Analysis in RCC Structures of Rigid Joint. *Journal of Mechanical and Civil Engineering*, 11(1), pp. 60-68.
- ETABS, 2017. CSI Analysis Reference Manual. *America: CSI*.
- Haque, M., 2021. Simplified Analytical Analysis of Fundamental Time of Structures. *Journal of Structural Engineering, its Applications and Analysis*, 4(2), pp. 1-24.
- Lin, L. *et al.*, 2013. Selection of seismic excitations for nonlinear analysis of reinforced concrete frame buildings. *Canadian Journal of Civil Engineering*, 40(5).
- Narsing, P. L. & Sharma, A., 2016. Nonlinear Time History Analysis of Reinforced Concrete Buildings with Floating Columns under Lateral and Vertical Component of Earthquake. *International Journal for Scientific Research & Development*, 4(7), pp. 795-797.
- Patil, R. & Pawar, V., 2020. Response Spectrum Analysis and Comparison of Seismic Parameters of Low-rise, High-rise and Asymmetrical RC Structure with and without Infill for Different Bay Dimensions. *International Research Journal of Engineering and Technology (IRJET)*, 7(7), pp. 642-647.
- Pauley, T. & Priestly, M. J. N., 1992. Seismic Design of Reinforced Concrete and Masonry Buildings. New York, U.S.A.: John Wiley and Sons.
- Tran, Q. H. *et al.*, 2018. Comparative Study of Nonlinear Static and Time-History Analyses of Typical Korean STS Container Cranes. *Advances in Civil Engineering*, pp. 1-13.